Conceptual and Computational Perspectives of Sustainable Rail Geotechnics

Buddhima Indraratna[1,*], Yujie Qi[2], Trung Ngo[3], Rakesh Malisetty[4], and Cholachat Rujikiatkamjorn[5]

[1] Distinguished Professor, Director of Transport Research Centre (TRC), University of Technology Sydney (UTS), 15 Broadway, Ultimo NSW 2007, Australia
buddhima.indraratna@uts.edu.au

[2] Senior Lecturer, Program Co-leader, Transport Research Centre (TRC), University of Technology Sydney (UTS), 15 Broadway, Ultimo NSW 2007, Australia
yujie.qi@uts.edu.au

[3] Senior Lecturer, Transport Research Centre (TRC), University of Technology Sydney (UTS), 15 Broadway, Ultimo NSW 2007, Australia
trung.ngo@uts.edu.au

[4] Postdoctoral research fellow, Transport Research Centre (TRC), University of Technology Sydney (UTS), 15 Broadway, Ultimo NSW 2007, Australia
RakeshSai.Malisetty@uts.edu.au

[5] Professor, Program Leader, Transport Research Centre (TRC), University of Technology Sydney (UTS), 15 Broadway, Ultimo NSW 2007, Australia
Cholachat.Rujikiatkamjorn@uts.edu.au

Abstract Given the rapidly evolving national policies of many countries which actively promote the socio-economic and environmental perspectives of circular economy, the Transport Research Centre at the University of Technology Sydney has launched innovative measures of adopting off-the-road rubber tyres, recycled rubber derivatives and granular by-products from mining and steel industry in novel track design. This paper presents some salient features evolving through mathematical formulations and numerical modelling of ballasted tracks incorporating recycled wastes, with special reference to: (i) a coupled rheological and continuum mechanics approach to predict a more accurate track dynamic response to evaluate the most suitable speeds and axle loads for specific substructure conditions with rubber inclusions, (ii) hybrid Discrete-Finite Element Method (DEM-FEM) simulations to micro-mechanically characterize ballast behavior with and with-out recycled rubber mats with a particular focus on ballast breakage. These computational modelling processes were calibrated and validated through comprehensive laboratory and field tests. The research outcomes provide a deeper understanding of the geotechnical effectiveness and performance enhancement of novel ballast tracks that incorporate blended waste materials.

Keywords: ballasted track, coupled rheological-continuum model, discreet-finite element modelling, impact loading, recycled rubber, track dynamic response

1 Introduction

With increasing demand and greater expectations for improved efficiency of railway operations with faster and heavier trains, more innovative design and construction methods for ballasted tracks are required to minimise track degradation and reduce maintenance costs. More importantly, since the net zero emission policy has been embraced in many countries, perspectives of sustainability and the circular economy have been the main themes of many geotechnical projects. Australia aims to complete the transition to net zero greenhouse emissions by 2050. To fulfil this target, one of the main solutions is to substantially reduce emissions from the source by implementing waste materials in transport infrastructure projects.

Recycled or marginal granular materials (e.g. recycled glass, waste rubber, construction and demolition materials, and mining by-products) have already been investigated or adopted by civil engineering. For instance, medium and fine recycled glass was found to have similar geotechnical properties as natural aggregates of sand, and could be used as road and other construction materials (Disfani et al., 2011, Mohajerani et al., 2017). The shear strength of the construction and demolition waste was investigated by Arulrajah et al. (2014), who found it to be suitable for pavement base and subbase applications. By-products from mining and manufacturing industry (e.g. steel furnace slag, coal wash, fly ash and bottom ash) have been adopted in various geotechnical applications, for instance as road base/subbase. Mixtures of coal wash and steel furnace slag were compacted in Port Kembla reclamation (Chiaro et al., 2015); a synthetic energy absorbing layer (SEAL) was developed by the 1st Author and his co-workers by mixing rubber crumbs, coal wash, and steel furnace slag in various proportions for railway sub-ballast/capping layers (Indraratna et al., 2018, Tawk et al., 2021, Hunt et al., 2022, Malisetty et al., 2022).

Among these novel sustainable applications, the use of recycled rubber from waste tyres or conveyor belts has become increasingly popular for railways. This is because the high energy absorbing and damping properties of rubber help to reduce the damage from the moving train loads to the track substructures. There are numerous applications of recycled rubber used in rail tracks. For instance, (i) recycled tyres after removing one side wall could be infilled with other recycled aggregated to be used as a capping layer to control lateral displacement and increase the load-bearing capacity of track (Indraratna et al., 2022); (ii) large rubber granulates (9.5-16mm) were mixed with ballast particles to serve as the bottom ballast layer, which was found to efficiently mitigate ballast breakage and settlement under dynamic train loads simulated via larger-scale triaxial testing and trialed in the field (Sol-Sánchez et al., 2015, Arachchige et al., 2023, Indraratna et al., 2024); (iii) rubber geogrids made from recycled conveyor belts using water jet cutting technology was installed at the interface of ballast and sub-ballast to increase the particle interlocking, reduce lateral movement, as well as mitigate ballast degradation (Hettiyahandi et al., 2024, Qi et al., 2024); and (iv) rubber mats including under ballast mats or under sleeper pads were found beneficial to reduce the impact

loading and ballast breakage (Sol-Sánchez et al., 2014, Indraratna et al., 2020b, Indraratna et al., 2021).

Although comprehensive laboratory and field tests indicate the promising performance of the railway incorporating these novel rubber inclusions, there are very limited predictive models for rubber inclusions from a mathematical or fundamental perspective. In view of the above, this paper provides two computational methods to simulate the behaviour of these energy-absorbing rubber materials under dynamic and impact loading. Firstly, a coupled rheological-continuum model is proposed to investigate the dynamic responses (critical speed, stress distribution and deflection) of the track with the presence of a synthetic energy absorbing layer (SEAL; a mixture of rubber crumbs with steel furnace slag and coal wash). Secondly, a coupled discrete-finite element model (DEM-FEM) will be developed to investigate the mechanism of using rubber mats to mitigate ballast degradation under impact loading.

2 Analytical Modelling of Railway Track

In this section, a coupled rheological-continuum model is presented to understand the dynamic response of the track under different subgrade and operational conditions. Though several methods are available to estimate the track dynamic responses, analytical models are often user-friendly and simple, yet effective in capturing the influence of moving trains on the stress distribution and degradation response of track substructure. As shown in Fig. 1, the analytical model presented in this paper combines the track superstructure (i.e., rail, rail pads and sleepers) using rheological elements with the track substructure (i.e., ballast, capping, and subgrade) modelled as a continuum layered half-space. A continuum half-space allows the model to capture the dispersion of Rayleigh waves, thereby simulating the influence of R-wave propagation on the dynamic stresses and displacements in the track layers as can be seen in Fig. 1.

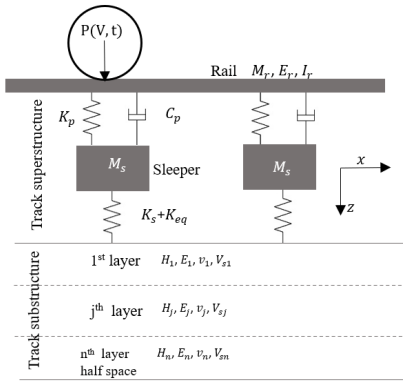

Fig. 1 Schematic of the railway track superstructure and substructure used for the analytical model

The equations of motion for track superstructure system subjected to a moving axle load P travelling at a speed V can be represented using the following equations:

$$E_r I_r \frac{\partial^4 u_r}{\partial x^4} + M_r \frac{\partial^2 u_r}{\partial t^2} + C_p \frac{\partial u_r}{\partial t} + K_p(u_r - u_s) = P(t,V) \quad (1)$$

$$K_p(u_s - u_r) - M_s \frac{\partial^2 u_r}{\partial t^2} + K_{eq} u_s = 0 \quad (2)$$

where, E_r, I_r represent the Youngs modulus of rail, u and t denote displacement and time, K, C and M represents stiffness, damping and mass, respectively, while the subscripts r, p and s indicate rail, rail pads, and sleeper, respectively. K_{eq} is the equivalent stiffness contributed by the substructure system, which according to Mezher et al. (2016) can be ignored for a more simple numerical analysis without compromising the outcomes.

The dynamic load from the superstructure system is transferred to the substructure system which propagates along the surface in the form of Rayleigh waves. Due to the nonhomogeneous nature of the substructure system with distinct layers such as ballast, capping and subgrade, the R-waves are generated at different frequencies causing dispersion of waves. Following the methodology proposed by Suiker et al., (1999), the Cauchy stresses in the vertical, longitudinal and shear directions and transient displacements caused by the propagation of R-waves in the j^{th} track layer can be given by the following equations, with their detailed derivations available in Malisetty and Indraratna (2024):

$$\sigma_{zz}^j = e^{i(\omega t - kx)}\left\{b_{1j}A_{p1}^j e^{i\xi_{p1}^j Z} + b_{2j}A_{s1}^j e^{i\xi_{s1}^j Z} + b_{1j}A_{p2}^j e^{i\xi_{p2}^j Z} - b_{2j}A_{s2i}^j e^{i\xi_{s2}^j Z}\right\} \quad (3)$$

$$\sigma_{xx}^j = e^{i(\omega t - kx)}\left\{b_{3j}A_{p1}^j e^{i\xi_{p1}^j Z} - b_{2j}A_{s1}^j e^{i\xi_{s1}^j Z} + b_{3j}A_{p2}^j e^{i\xi_{p2}^j Z} + b_{2j}A_{s2}^j e^{i\xi_{s2}^j Z}\right\} \quad (4)$$

$$\sigma_{zx}^j = e^{i(\omega t - kx)}\left\{b_{4j}A_{p1}^j e^{i\xi_{p1}^j Z} + b_{5j}A_{s1}^j e^{i\xi_{s1}^j Z} - b_{4j}A_{p2}^j e^{i\xi_{p2}^j Z} + b_{5j}A_{s2}^j e^{-i\xi_{s2}^j Z}\right\} \quad (5)$$

$$u_x^j = -ie^{i(\omega t - kx)}\left\{kA_{p1}^j e^{i\xi_{p1}^1 Z} + kA_{p2}^1 e^{i\xi_{p2}^1 Z} + \xi_{s1}^1 A_{s1}^1 e^{i\xi_{s1}^1 Z} - \xi_{s2}^1 A_{s2}^1 e^{i\xi_{s2}^1 Z}\right\} \quad (6)$$

$$u_z^j = ie^{i(\omega t - kx)}\left\{\xi_{p1}^1 A_{p1}^1 e^{i\xi_{p1}^1 Z} - \xi_{p2}^1 A_{p2}^1 e^{i\xi_{p2}^1 Z} - kA_{s1}^1 e^{i\xi_{s1}^1 Z} - kA_{s2}^1 e^{i\xi_{s2}^1 Z}\right\} \quad (7)$$

In Eqs. (3)-(7), z represents the depth of the measurement from the surface of the ballast layer, A_p and A_s are the amplitude of compression (P-) and Shear (S-) waves, respectively. b_{1j} to b_{5j} are the coefficients represented as a function of elastic modulus and Poisson's ratio of ballast and subgrade layers. ω and k are the angular frequency and wave number of the R-waves, respectively, and $\xi_{p,s,1,2}^j$ represent the depth attenuation factor for P and SV waves given as:

$$\xi_{p,s,1,2}^j = = \pm\sqrt{\frac{\omega^2}{C_{p,s}^{j\ 2}} - k^2} \quad (8)$$

where, C_p^j and C_s^j are the P- and SV-wave velocities in the j^{th} layer, respectively. To solve for the unknown amplitude parameters, compatibility conditions at the boundaries of each layer are considered. At the surface of the ballast layer, the vertical stress is equal to the dynamic stress transmitted from the sleeper $\left(\frac{P_{tr}}{A_{sl}}\right)$, while the shear stresses are equal to zero. At all other layer interfaces, the stress and displacement compatibility conditions are followed.

For applying the abovementioned conditions to a 3-layered substructure consisting of ballast, capping and subgrade (half space), the stress and displacement equations can be transformed into $MA = q$. A is the amplitude vector and M is a 10x10 matrix consisting of coefficients which are functions of ω, k, elastic properties of substructure layers and the thickness of each layer. The numerical solution can be determined by taking the product of the inverse of M and q. Equating the determinant of M to 0 gives the dispersion curves for the track substructure which is representative of the maximum amplitudes of the R-wave.

2.1 Model performance

The model was used to predict dispersion curves, transient displacements and vertical stresses and compared with field data acquired from different studies. For analysis, 60kg rail based on UIC standard (international union of railways) had $E_r I_r$ = 63x10^5 Pa.m^4, K_p and C_p were 5x10^8 N/m and 2.5x10^5 N.s/m, respectively, while M_s and K_s were 490 kg and 60x10^6 N/m, respectively. For the dispersion curves and vertical stress response, a non-destructive site investigation previously conducted by the authors at a field site in Chullora (western suburb of Sydney) was adopted (Malisetty and Indraratna, 2024). Fig. 2a shows the fundamental mode of the dispersion curve predicted by the model for track conditions at Chullora which closely matches that of the field-measured dispersion curve. Based on the work by Connolly et al. (2014), the dispersion curves of the superstructure and substructure are intersected which yielded a critical speed of 198 m/s. The high critical speed values can be attributed to a stiff subgrade (weathered shale) presented at the site at a shallow depth of 1.3m below the sleeper base.

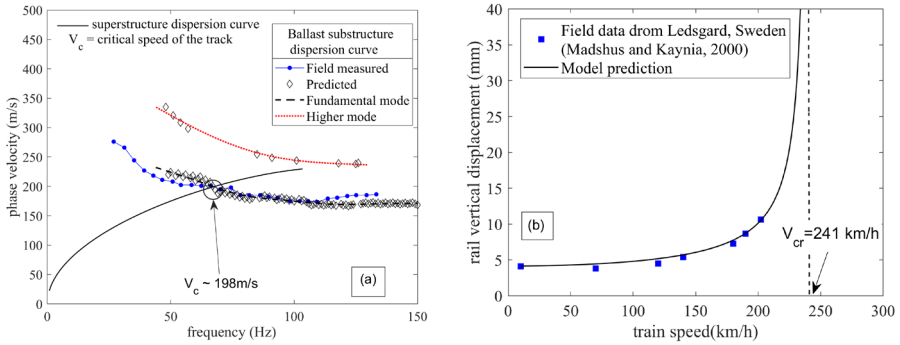

Fig. 2 Comparison of model predictions with field measurements (a) track dispersion curves (b) dynamic vertical rail displacements at different train speeds

Fig. 2b shows the vertical rail displacements predicted at different train speeds for the high-speed rail site at Ledsgard, Sweden (Madshus and Kaynia, 2000) compared with the measured values. The model parameters for both sites are shown in Table 1, and for simplicity, different subgrade layers are combined to be considered as an equivalent subgrade. It is demonstrated that the model captures the amplification of dynamic displacements with increasing train speeds, quite well with the measured data. As predicted by Kaynia et al. (2000), the critical speed at the site was 235 km/h, which is close to that predicted by the model (241 km/h).

Table 1 Material properties

Ledsgard, Sweden (Madshus and Kaynia, 2000)								
	E (MPa)	v	ρ (kg/m^3)	H (m)	-	-	-	-
Crust	22.35	0.49	1500	1.1	-	-	-	-
Organic clay	6	0.49	1260	3	-	-	-	-
Clay-1	15.8	0.49	1475	4.5	-	-	-	-
Clay-2	31	0.49	1475	6	-	-	-	-
Clay-3	44	0.49	1475	HS	-	-	-	-
Field studies (carried out in Australia)								
	Chullora, NSW (Malisetty and Indraratna 2024)				Bulli, NSW, Australia (Indraratna et al., 2010)			
	E (MPa)	v	ρ (kg/m3)	H (m)	E (MPa)	v	ρ (kg/m^3)	H(m)
Ballast	150	0.35	1660	0.3	150	0.35	1660	0.3
Capping	182	0.3	1800	0.2	180	0.3	1800	0.15
Fill	127.4	0.4	2000	0.5	-	-	-	-
Subgrade	320	0.24	2000	HS	50	0.4	2000	HS

2.2 Effect of recycled materials on critical speed

The dynamic response of the track such as stresses and displacements and the subsequent degradation of subgrade is dependent on the proximity of the operating train speed to the critical speed of the track. By using a capping layer made of compacted granular fill, the critical speed of the track can be increased. However, as discussed earlier, the use of sustainable materials, such as SEAL with recycled rubber, is becoming increasingly important compared to traditional quarried materials. In this section, the present model is extended to predict subgrade degradation under repeated railway loading at different speeds and axle loads, while providing information on the effectiveness of recycled materials in alleviating/retarding subgrade degradation. For this, a track having a moderately soft subgrade was considered, similar to that of the rail line in the town of Bulli south of Sydney (Indraratna et al., 2010) with material properties shown in Table 1. Notably, several incidents of mud pumping were recorded

on that track section caused by subgrade degradation exacerbated by drainage impediments. The degradation curve as shown in Eq. (9) obtained from controlled laboratory experiments on subgrade soils consisting of silty clays with a dry density of 1710 kg/m^3 was adopted (Nguyen et al., 2021). The relationship represents the degradation (δ) of the shear modulus of subgrade soil (G) with number of loading cycles (N) and cyclic stress ratio (CSR=$\frac{q_{oct}}{2\sigma_c'}$).

$$1 - \delta = G_{sN}/G_{s1} = 1 - \log(a\,.CSR)^b\,[\log N]^c \tag{9}$$

where, a, b and c are empirical constants and are considered as 3.34, 0.69 and 2.5, respectively, q_{oct} is the maximum octahedral deviator stress, and σ_c' is the effective confining pressure.

Fig. 3a shows the variation of the dynamic amplification factor of octahedral stress in the subgrade, approximately 100 mm below the top surface of the subgrade when different capping layers are used and when subgrade degradation is ignored. Octahedral stress is used for Dynamic Amplification Factor (DAF) as increased train speeds cause not only amplification of vertical stresses, but also amplification of shear and longitudinal stresses, and thus using q_{oct} is more appropriate. For comparison, DAF=1 is benchmarked to q_{oct} at the same point in the subgrade when no capping is used. Two key observations can be made from Fig. 3a: (i) increase in critical speed of the track when capping layer of different thickness and different materials are used, and (ii) DAF reduced with the addition of capping layers at both low train speeds as well as train speeds close to critical speeds. Although the SEAL layer is not as effective as the traditional capping layer due to lower shear modulus compared to that of traditional capping, using a 200mm SEAL [$E = 95\ MPa$] (Qi et al., 2018)], it still provides similar advantages as 150mm traditional capping layer. However, it is to be noted that the subgrade condition does not remain the same throughout the operational period of the track. When the subgrade is saturated and with low drainage potential such as during excessive rainfall events, the subgrade can degrade leading to excessive amplification than expected, leading to exacerbated problems such as mud pumping.

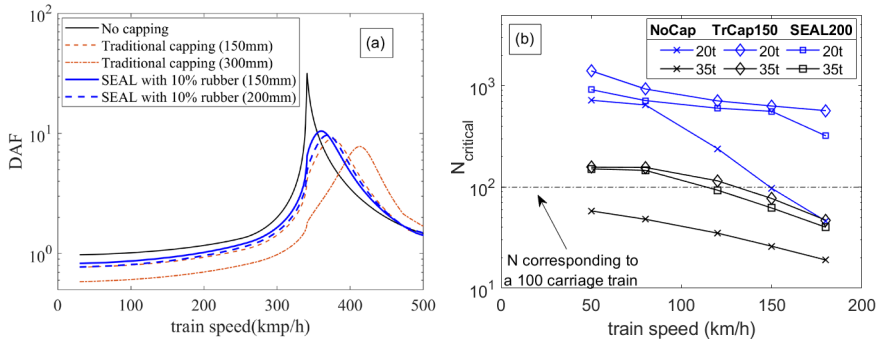

Fig. 3 Influence of different capping layers on (a) Dynamic amplification factor of stresses at 100mm below the surface of subgrade (b) critical number of loading cycles considering subgrade degradation

Fig. 3b provides information on the critical number of loading cycles that a train can run on a track built on a problematic subgrade under unfavorable conditions. For calculating the N_{crit}, q_{oct} at 1m depth below the sleeper base as per the analytical model for each cycle and then combined by Eq. (9) until the degradation of the subgrade reaches 60%. This threshold value is considered as the degradation of subgrade increases rapidly as observed from experimental results (Nguyen et al., 2021) and can act as an early warning sign to identify critical subgrade condition. For comparison, the track without a capping layer is plotted against the track with 150mm traditional capping and 200mm SEAL layer. As can be seen from Fig. 3b, N_{cr} reduces with increasing train speed as well as increasing axle loads for all geometry and axle load cases. For passenger trains (maximum axle load of 20 tonnes), as expected, a higher N_{cr} of more than 700 cycles is observed for low train speeds. In contrast, this is reduced by less than 100 cycles for high train speeds. However, since passenger trains comprise limited carriages, they pose no threat to subgrade degradation. Nevertheless, it can be observed that the critical number of load cycles is increased by using a 150mm thick traditional capping or a 200mm thick SEAL with recycled materials, though the degree of improvement using both materials is almost the same. Importantly, for higher axle loads, for example 35-tonne axle loads which are common in freight networks of most countries, N_{cr} for track without a capping layer is less than 100 cycles even at the lower train speeds. This is especially critical for freight trains as most freight trains are very long, with no rest period for the excess pore water pressures in the subgrade to dissipate. Improvement in N_{cr} is observed by adding capping layers, but the subgrade still reaches the threshold degradation quicker within 100 cycles (N_{cr}<100 cycles), when the train speed is beyond 110 km/h.

3 Numerical Modeling of Recycled Rubber Mat-Reinforced Ballast under Impact Load

Railway operations continue to face major issues in managing track settlement, predominantly caused due to ballast breakage (Le Pen et al., 2016, Indraratna et al., 2019). Prior research demonstrated that cellular reinforcements, such as geocells, and planar polymeric geogrids can improve track stability (Brown et al., 2007, Biabani et al., 2016, Luo et al., 2023). Nevertheless, a significant drawback of traditional geogrids positioned underneath the ballast layer is their inability to offer enough damping to absorb impact loads caused by rail corrugation or defective wheels (Indraratna et al., 2020a). Rubber mats were recently trialed to improve track stability and lessen ballast breakage and distortion (Sol-Sánchez et al., 2014). Test results showed that the use of rubber materials, such as under-sleeper mat (USP) at the ballast-sleeper interface or under-ballast mat (UBM) installed beneath the ballast, can effectively reduce the stress transmitted to the track substructure (Jayasuriya et al., 2019).

In order to lessen the adverse effects of impact loads on ballasted tracks, this section explores the application of recycled rubber mats (RM) to be placed under the ballast layer. A number of tests were carried out utilizing the impact testing facilities, as

detailed by Remennikov and Kaewunruen (2014). The test results highlight that placing a rubber pad underneath the ballast layer significantly reduces the fracture of the ballast particles. While comprehensive laboratory test results were reported by Ngo et al., (2019), this paper revisits some of these findings to bolster the performance of the recycled rubber mat through numerical investigation as described below.

3.1 Numerical modelling of impact test

A common approach for examining the micro-mechanical behaviour of aggregates is the discrete element method, DEM, which was initiated by Cundall and Strack (1979), and this method has been commonly adopted for granular materials (McDowell and Harireche, 2002, O'Sullivan and Cui, 2009, Jia et al., 2023). DEM provides in-depth information on phenomena that are frequently challenging to capture using continuum-based techniques, such as breakage, irregular grain geometries, contact force distributions, and the link between macro and micro-scale features. The performance of aggregates under impact loads was investigated using DEM, with a focus on the impact of recycled rubber mat (RM). In this study, a sample of ten ballast particles was gathered and scanned with a 3D laser scanner to precisely capture the irregular shapes of the particles. As shown in Fig. 4a, the scanned data was processed to produce polygonal meshes that mimic the angularity and geometric characteristics of ballast. To create the ballast inside the DEM framework, subroutines were simulated using the FISH programming language (Itasca, 2020). In order to fill the digital meshes, these particles were modelled by joining several spheres together; and by permitting these bonds to fail (break), the ballast breakage was roughly replicated.

The continuum modeling method is effective for simulating large deformations but neglects the effects of angularity and particle breakage. The Discrete-Finite Element Method (DEM-FEM), a linked discrete-continuum strategy, is often used to overcome this constraint by combining the benefits of both numerical techniques (Indraratna et al., 2020a). In this study, the continuum approach was adopted to describe the rubber membrane, i.e. rubber mat, capping and encircling of the ballast assembly (Fig. 4b, 4c), and DEM was adopted to model aggregates. A shape function was used to determine the velocities and positions of the membrane's edge-connected faces. By determining contact forces at the facets and applying the force equilibrium at their vertices, the coupling between DEM and FEM could be facilitated. Stiffness contributions were then taken into account when these forces were delivered to the nodes. To simulate impact force, a hammer was simulated as a rigid body that can be dropped from different heights in Fig. 4d. For additional information about the input parameters and coupling model used in this study, please refer to Ngo et al. (2024).

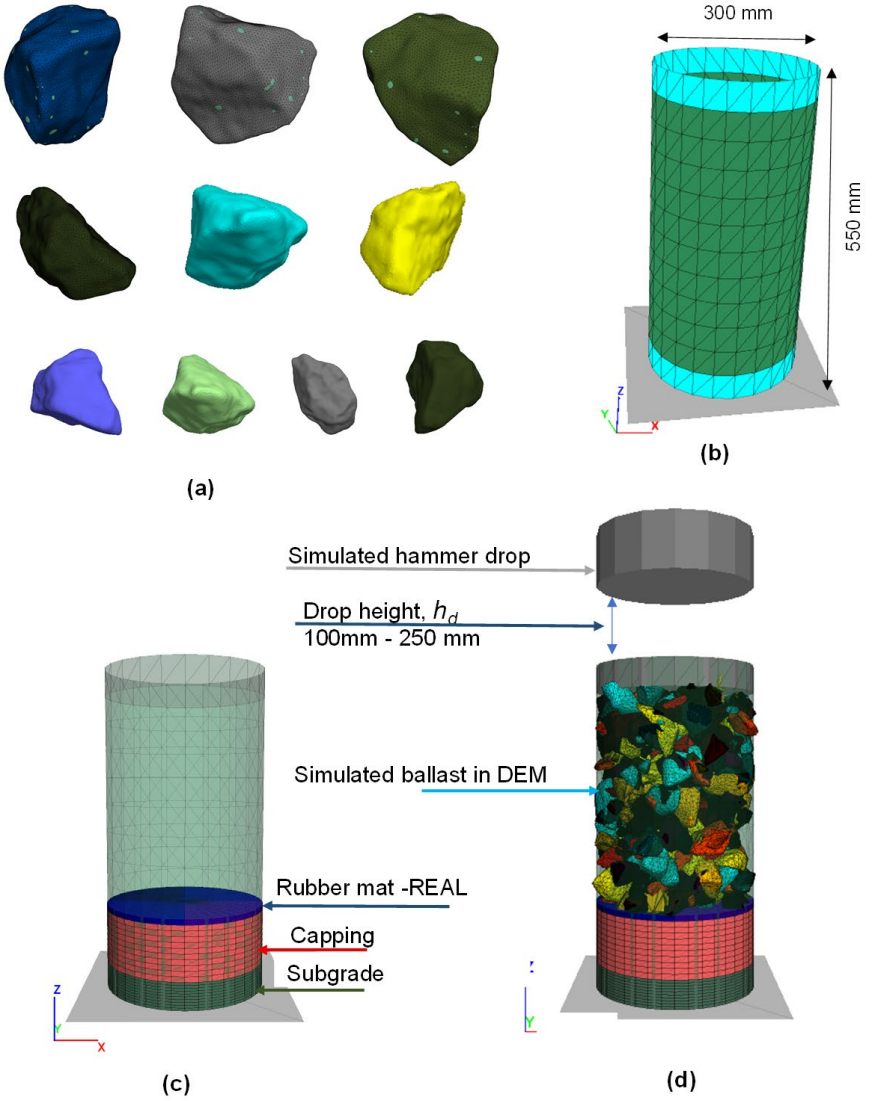

Fig. 4 (a) Discretised ballast particles in DEM; (b) Model geometry; (c) Placement of rubber mat, capping and subgrade; (d) DEM model for impact test (Ngo et al., 2024)

3.2 The role of rubber mat in mitigating impact force

The impact forces measured experimentally with a recycled rubber mat (RM) subjected to a drop height of h_d = 150 mm and those anticipated using DEM are presented in Fig. 5. With a distinctive pattern of several peaks (P_1 force) followed by a protracted, lower-magnitude peak (P_2 force), the simulated forces closely match the experimental findings.

The system's acceleration from strong inertial forces causes the P_1 force to arise when the hammer strikes the ballast (Fig. 5a), peaking sharply at about 247 kN during a short period of 10 ms. Subsequently, several secondary peaks (P_2) are seen, which finally taper off to about 30-40 kN. Although the force pattern is identical when the RM is included (Fig. 5b), it significantly lowers the intensity of the initial peak (P_1). The peak force was approximately 247 kN without the RM and reduced to about 158 kN with the RM, indicating a reduction of around 36%. The energy absorption capability of the rubber mat (RM), which dissipates a portion of the impact force through its compressive qualities, is responsible for this notable drop.

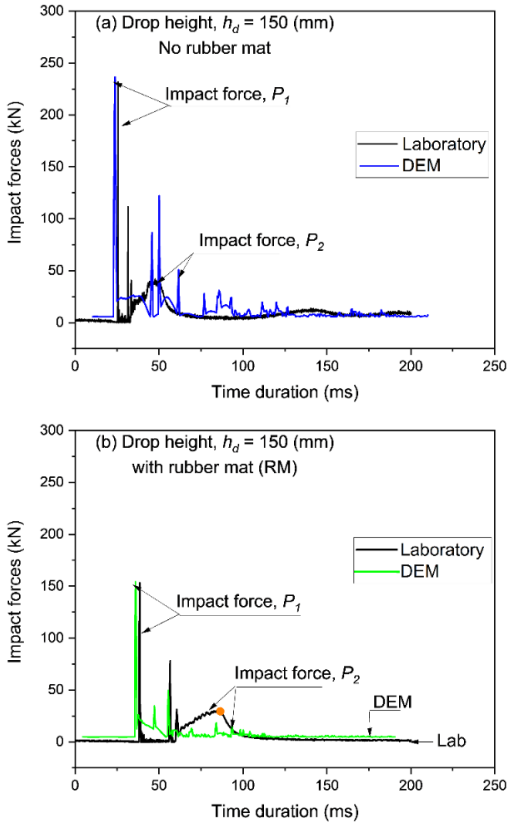

Fig. 5 Predicted impact forces from DEM and laboratory measurements: (a) without RM and (b) with RM. (modified after Ngo et al. 2024)

3.3 Effect of rubber mats on reducing particle breakage

In the current DEM analysis, several spheres were bonded together to fill the digitised mesh to represent ballast particles; the breaking of these bonds was adopted to simulate ballast breakage. Fig. 6 illustrates the accumulation of broken bonds ($N_{Breakage}$) as a function of the number of drops, N_{drop} at a drop height of h_d=200 mm. For comparison, the laboratory-measured ballast breakage index (BBI) was also included. The results show that $N_{Breakage}$ increases with rising N_{drop}, closely following the trends of the laboratory-measured BBI. The energy-absorbing capacity of RM is responsible for the considerable reduction in Breakage $N_{Breakage}$. By absorbing a portion of the impact energy, the rubber mat lessens the impact force applied to the ballast and thereby prevents damage. Additionally, RM reduces the magnitude of contact forces on the ballast by facilitating more even force distributions over a wider region.

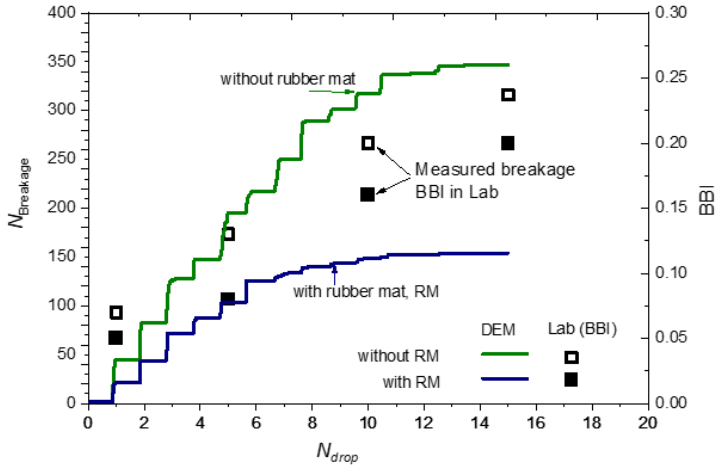

Fig. 6 Variations of broken bonds ($N_{Breakage}$) and the ballast breakage index (BBI) during impact tests (modified after Ngo et al., 2024)

4.4 Evolution of Coordination Number (Cn)

The average number of contact forces in a particle is represented by the coordination number, C_n which is a microscopic parameter used to describe particle packing (Soga and O'Sullivan, 2010). Changes in packing and the new contacts created during the loading and particle breakage influence the development or loss of contacts, as shown by variations in C_n presented in Fig. 7. According to the results, C_n drops after the hammer hits the ballast assembly and then slightly rises as N_{drop} proceeds before stabilizing at the test's conclusion. When RM is used, values of C_n fluctuate around 6.62

and is comparatively constant throughout the test. Without RM, on the other hand, C_n shows considerable oscillations (C_n =6.35 to 6.6), most likely as a result of particle breakage that causes particle displacement, rearrangement, and the creation of new connections. A higher C_n (6.62 with RM compared to 6.51 without RM) is the outcome of including RM. This implies in practice that a greater C_n can improve the constraint on particle's deformation and lower breakage.

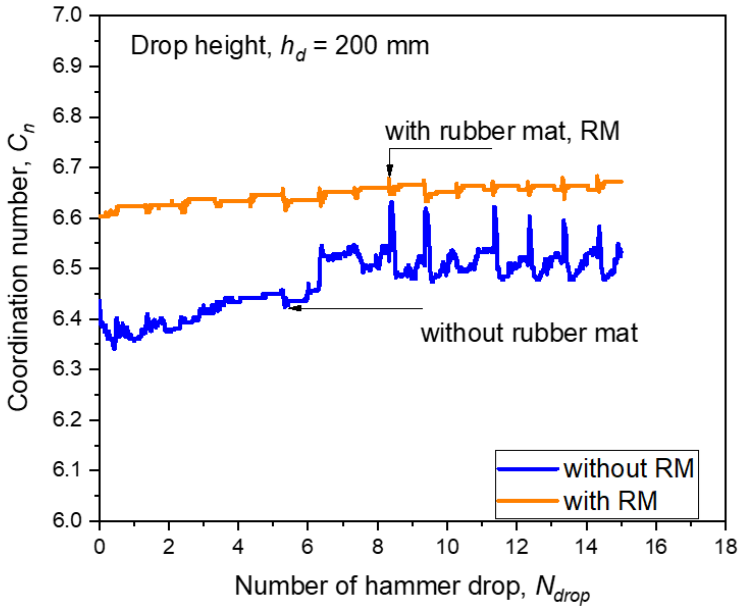

Fig. 7 Effect of rubber mat on C_n for a drop height, h_d =200 mm (modified after Ngo et al., 2024)

4 Conclusions

This paper introduced two computational methods to investigate the rail track performance with different substructure conditions, especially with recycled materials (e.g. SEAL and rubber mats). A coupled rheological-continuum model was developed to understand the track dynamic responses and the DEM-FEM method was used to investigate the influence of adding rubber mats on the track performance under impact loading. Key findings include:

- The addition of a capping layer increased the rail track's critical speed and reduced the DAF. The track having a softer SEAL with a thickness of 200 mm performs comparable to that with conventional capping materials of 150 mm. Under unfavorable conditions with problematic subgrade (e.g. saturated subgrade with low drainage conditions), the critical number of loading cycles

that the track could resist without subgrade instability is reduced with increasing train speed and axle loads, owing to the amplification of dynamic stresses. This critical number increased significantly with the addition of a capping layer, which delayed subgrade degradation and enabled 35-tonne axle trains to operate at speeds of up to 100 km/h. This finding amply reflects the importance of using a capping layer in railways under heavy haul trains, although a higher capping thickness is needed when using softer and sustainable energy-absorbing materials for new track design and construction.

- Impact force intensity was considerably decreased by the addition of rubber mat (RM). The peak impact force dropped by about 36% with RM (drop from 247 kN about 158 kN with RM). The use of rubber matconsiderably decreased the $N_{Breakage}$ by about 34%. For instance, at N_{drop} = 15, $N_{Breakage}$ was 248 with RM and 374 without it. Furthermore, the presence of RM increased the C_n, which was C_n = 6.62 with RM compared to C_n = 6.51 in the absence of it. This finding leads to the conclusion in practice that, adding recycled rubber mats for track substructure can reduce the impact loads, decrease particle breakage and improve track stability, which eventually reduces track maintenance expenses related to ballast tamping.

Acknowledgements The authors would like to thank the financial support from the Australian Research Council (ARC) Linkage and Discovery projects, namely, ARC-LP200200915 and ARC-DP220102862. The authors would also like to acknowledge the financial and technical support from industry partners including Sydney Trains, SMEC Australia, Bentley Systems and Bestech Australia. Some figures were reproduced from the authors' past publications published in journals such as Géotechnique and Transportation Geotechnics, with kind permissions from ICE and Elsevier, respectively.

References

Arachchige, C. M., Indraratna, B., Rujikiakamjorn, C., Qi, Y. and Siddiqui, A. R. (2023). Use of waste rubber inclusions for ballasted railway construction–A real-life case study. Smart Geotechnics for Smart Societies, CRC Press**:** 2567-2570.

Arulrajah, A., Disfani, M. M., Horpibulsuk, S., Suksiripattanapong, C. and Prongmanee, N. (2014). "Physical properties and shear strength responses of recycled construction and demolition materials in unbound pavement base/subbase applications." *Construction and Building Materials* 58: 245-257.

Biabani, M. M., Indraratna, B. and Ngo, N. T. (2016). "Modelling of geocell-reinforced subballast subjected to cyclic loading." *Geotextiles and Geomembranes* 44(4): 489-503.

Brown, S. F., Kwan, J. and Thom, N. H. (2007). "Identifying the key parameters that influence geogrid reinforcement of railway ballast." *Geotextiles and Geomembranes* 25(6): 326-335.

Chiaro, G., Indraratna, B., Tasalloti, S. A. and Rujikiatkamjorn, C. (2015). "Optimisation of coal wash–slag blend as a structural fill." *Proceedings of the Institution of Civil Engineers-Ground Improvement* 168(1): 33-44.

Connolly, D., Kouroussis, G., Woodward, P. K., Costa, P. A., Verlinden, O. and Forde, M. C. (2014). "Field testing and analysis of high speed rail vibrations." *Soil Dynamics and Earthquake Engineering* 67: 102-118.

Cundall, P. A. and Strack, O. D. L. (1979). "A discrete numerical model for granular assemblies." *Géotechnique* 29(1): 47-65.

Disfani, M., Arulrajah, A., Bo, M. and Hankour, R. (2011). "Recycled crushed glass in road work applications." *Waste management* 31(11): 2341-2351.

Hettiyahandi, S., Indraratna, B., Ngo, T., Qi, Y. and Arachchige, C. (2024). The Effect of Recycled-Rubber Energy Absorbing Grids on the Performance of Railway Ballast: A Review. International Conf. on Transportation Geotechnics, Springer. https://doi.org/10.1007/978-981-97-8229-1_3

Hunt, H., Indraratna, B. and Qi, Y. (2022). "Ductility and energy absorbing behaviour of coal wash–rubber crumb mixtures." *International Journal of Rail Transportation* 11(4): 508-528.

Indraratna, B., Arachchige, C. M., Rujikiatkamjorn, C., Qi, Y. and Heitor, A. (2024). "Utilization of Granular Wastes in Transportation Infrastructure." *Geotechnical Testing Journal* 47(1): GTJ20220233.

Indraratna, B., Ngo, T. and Rujikiatkamjorn, C. (2020a). "Performance of Ballast Influenced by Deformation and Degradation: Laboratory Testing and Numerical Modeling." *International Journal of Geomechanics* 20(1): 04019138.

Indraratna, B., Nimbalkar, S., Christie, D., Rujikiatkamjorn, C. and Vinod, J. (2010). "Field assessment of the performance of a ballasted rail track with and without geosynthetics." *Journal of geotechnical and geoenvironmental engineering* 136(7): 907-917.

Indraratna, B., Qi, Y. and Heitor, A. (2018). "Evaluating the properties of mixtures of steel furnace slag, coal wash, and rubber crumbs used as subballast." *J. of Materials in Civil Engineering* 30(1): 04017251.

Indraratna, B., Qi, Y., Jayasuriya, C., Rujikiatkamjorn, C. and Arachchige, C. M. (2021). "Use of Recycled Rubber Inclusions with Granular Waste for Enhanced Track Performance." *Transportation Engineering*: 100093.

Indraratna, B., Qi, Y., Malisetty, R. S., Navaratnarajah, S. K., Mehmood, F. and Tawk, M. (2022). "Recycled materials in railroad substructure: an energy perspective." *Railway Engineering Science* 30: 304-322.

Indraratna, B., Qi, Y., Ngo, T. N., Rujikiatkamjorn, C., Neville, T., Ferreira, F. B. and Shahkolahi, A. (2019). "Use of geogrids and recycled rubber in railroad infrastructure for enhanced performance." *Geosciences* 9(1). https://doi.org/10.3390/geosciences9010030.

Indraratna, B., Qi, Y., Tawk, M., Heitor, A., Rujikiatkamjorn, C. and Navaratnarajah, S. K. (2020b). "Advances in Ground Improvement Using Waste Materials for Transportation Infrastructure." *Proceedings of the Institution of Civil Engineers-Ground Improvement*: 1-44.

Itasca (2020). "Particle flow code, PFC3D." *Itasca Consulting Group, Inc., Minnesota*.

Jayasuriya, C., Indraratna, B. and Ngo, T. (2019). "Experimental study to examine the role of under sleeper pads for improved performance of ballast under cyclic loading." *Transportation Geotechnics* 19: 61-73.

Jia, Y., Zhang, J., Chen, X., Miao, C. and Zheng, Y. (2023). "DEM study on shear behavior of geogrid-soil interfaces subjected to shear in different directions." *Computers and Geotechnics* 156: 105302.

Kaynia, A. M., Madshus, C. and Zackrisson, P. (2000). "Ground vibration from high-speed trains: prediction and countermeasure." *Journal of geotechnical and geoenvironmental engineering* 126(6): 531-537.

Le Pen, L., Milne, D., Thompson, D. and Powrie, W. (2016). "Evaluating railway track support stiffness from trackside measurements in the absence of wheel load data." *Canadian Geotechnical Journal* 53(7): 1156-1166.

Luo, Z., Zhao, C., Cai, W., Gu, Q., Lin, W., Bian, X. and Chen, Y. (2023). "Full-scale model tests on ballasted tracks with/without geogrid stabilisation under high-speed train loads." *Géotechnique* 0(0): 1-15.

Madshus, C. and Kaynia, A. (2000). "High-speed railway lines on soft ground: dynamic behaviour at critical train speed." *Journal of Sound and Vibration* 231(3): 689-701.

Malisetty, R. S. and Indraratna, B. (2024). "Critical speed of ballasted railway tracks: Influence of ballast and subgrade degradation." *Transportation Geotechnics* 46: 101246.

Malisetty, R. S., Indraratna, B., Qi, Y. and Rujikiatkamjorn, C. (2022). "Shakedown response of recycled rubber–granular waste mixtures under cyclic loading". Géotechnique, 73(10):843-848.

McDowell, G. R. and Harireche, O. (2002). "Discrete element modelling of soil particle fracture." *Géotechnique* 52(2): 131-135.

Mezher, S. B., Connolly, D. P., Woodward, P. K., Laghrouche, O., Pombo, J. and Costa, P. A. (2016). "Railway critical velocity–Analytical prediction & analysis." *Transportation Geotechnics* 6: 84-96.

Mohajerani, A., Vajna, J., Cheung, T. H. H., Kurmus, H., Arulrajah, A. and Horpibulsuk, S. (2017). "Practical recycling applications of crushed waste glass in construction materials: A review." *Construction and Building Materials* 156: 443-467.

Ngo, T., Indraratna, B., Coop, M. and Qi, Y. (2024). "Behaviour of ballast stabilised with recycled rubber mat under impact loading." *Géotechnique* 0(0): 1-21. https://doi.org/10.1680/jgeot.23.00073

Ngo, T., Indraratna, B. and Rujikiatkamjorn, C. (2019). "Improved performance of ballasted tracks under impact loading by recycled rubber mats." *Transportation Geotechnics* 20: 100239.

Nguyen, T. T., Indraratna, B. and Singh, M. (2021). "Dynamic parameters of subgrade soils prone to mud pumping considering the influence of kaolin content and the cyclic stress ratio." *Transportation Geotechnics* 29: 100581.

O'Sullivan, C. and Cui, L. (2009). "Micromechanics of granular material response during load reversals: Combined DEM and experimental study." *Powder Technology* 193(3): 289–302.

Qi, Y., Indraratna, B., Heitor, A. and Vinod, J. S. (2018). "Effect of rubber crumbs on the cyclic behavior of steel furnace slag and coal wash mixtures." *Journal of Geotechnical and Geoenvironmental Engineering* 144(2): 04017107.

Qi, Y., Indraratna, B., Ngo, T., Arachchige, C. M. and Hettiyahandi, S. (2024). "Sustainable solutions for railway using recycled rubber." *Transportation Geotechnics*: 101256.

Remennikov, A. M. and Kaewunruen, S. (2014). "Experimental load rating of aged railway concrete sleepers." *Engineering Structures* 76: 147-162.

Soga, K. and O'Sullivan, C. (2010). "Modeling of geomaterials behavior." *Soils and Foundations* 50(6): 861-875.

Sol-Sánchez, M., Moreno-Navarro, F. and Rubio-Gámez, M. C. (2014). "Viability of using end-of-life tire pads as under sleeper pads in railway." *Construction and Building Materials* 64: 150-156.

Sol-Sánchez, M., Thom, N., Moreno-Navarro, F., Rubio-Gamez, M. and Airey, G. (2015). "A study into the use of crumb rubber in railway ballast." *Construction and Building Materials* 75: 19-24.

Suiker, A. S., Chang, C. S., de Borst, R. and Esveld, C. (1999). "Surface waves in a stratified half space with enhanced continuum properties. Part 1: Formulation of the boundary value problem." *European Journal of Mechanics-A/Solids* 18(5): 749-768.

Tawk, M., Qi, Y., Indraratna, B., Rujikiatkamjorn, C. and Heitor, A. (2021). "Behavior of a Mixture of Coal Wash and Rubber Crumbs under Cyclic Loading." *Journal of Materials in Civil Engineering* 33(5): 04021054.